Electronic Supporting Information

3D Printing of Reactive Macroporous Polymers via Thiol-Ene Chemistry and Polymerization-Induced Phase Separation

Nikolaj K. Mandsberg†, Fatma Aslan†, Zheqin Dong, Pavel A. Levkin
†These authors contributed equally.

Table of Contents

Materials

Pentaerythritol tetrakis(3-mercaptopropionate) (PETMP, Sigma-Aldrich, >95%), tri(ethylene glycol) divinyl ether (TEG, Sigma-Aldrich, 98%), 1,3,5-triallyl-1,3,5-triazine-2,4,6-(1H,3H,5H)-trione (TTT, Sigma-Aldrich, 98%), phenyl bis(2,4,6-trimethyl benzoyl)-phosphine oxide (Irgacure 819-BAPO, Hock), (2,2,6,6-Tetramethylpiperidine 1-oxyl) (TEMPO, Fluka), 1-(Phenyldiazenyl)naphthalen-2-ol (Sudan I, Sigma-Aldrich), and polyethylene glycol (PEG200). Mn = 200, Sigma-Aldrich), acetone (Merck, ≥ 99%), diethylene glycol diethyl ether (DGDE, Merck, ≥ 99%), Tetrahydrofuran (THF, Sigma-Aldrich, ≥ 99.9%), toluene (VWR, ≥ 99. 5%), 1-propanol (Merck), ethylene glycol (Acros), 1-decanol (Sigma-Aldrich, 98%), cyclohexanol (Merck), 2-propanol (Carl Roth), N,N-dimethylformamide (DMF, VWR, 99. N,N-dimethylacetamide (DMA, Merck), dimethyl sulfoxide (DMSO, VWR), 1H,1H,2H,2H-Perfluorodecyl acrylate (PFDA, Sigma-Aldrich, contains 100 ppm tert-butylcatechol as inhibitor, 97%), triethylamine (TEA, Alfa-Aesar, 98%), and hydroxyethylamine (HEA, Sigma-Aldrich, 98%). All materials were used as received.

Manufacturing

Resin preparation

The resins were prepared in black glass vials to protect them from UV light exposure. The three main ingredients, pentaerythritol tetrakis(3-mercaptopropionate) (PETMP), tri(ethylene glycol) divinyl ether (TEG), and porogen solvent (primarily investigated with polyethylene glycol 200 as the porogen), were combined in specific amounts. The photoinitiator Irgacure 819 was added at a concentration of 2% mol to thiol, along with Sudan I as an absorber (0.025 wt% of total ink) and (2,2,6,6-Tetramethylpiperidin-1-yl)oxyl (TEMPO) quencher (0.01 wt% of total ink). The mixture was vigorously mixed for 10 seconds and sonicated for 30 minutes at room temperature to ensure comprehensive and consistent mixing of the components. The resin was used for printing immediately after.

3D printing

For our 3D printing experiments, we utilized the Miicraft Prime 110, a commercial desktop DLP printer from Germany that uses a 385 nm LED projector as its light source. The light intensity at the tank was set to 1.0 mW cm−2, and the printer achieved an XY resolution of 40 µm. The printer's build area dimensions are 116 mm × 62 mm × 12 mm, which allows for layer thicknesses ranging from 5 to 500 µm to be adjusted. To optimize resolution and minimize layer delamination, we calibrated the exposure time and layer thickness. We used a layer thickness of 50 µm and an exposure time of 10 seconds for each layer, except for the base layer, which required a longer curing time of 60 seconds.

Residue removal

After the 3D printing process, the objects were detached from the metal build platform with care. Subsequently, they were submerged in acetone for a thorough cleaning process that lasted 24 hours. The volume ratio used for this step was between 20 to 50 times the volume of the printed object, ensuring the effective removal of the majority of unreacted crosslinkers and porogens. After the initial 24-hour period, fresh acetone was used for a final washing step. This crucial step ensured the complete removal of all residual materials from the 3D printed objects.

Post-modification

We modified certain structures through a chemical post-modification process. We altered the wettability properties of both external and internal surfaces by manipulating the type of reagent and the concentration of free thiol groups. Specifically, we used polymeric objects printed using OSTE-thiol formulations. The printed 3D objects underwent thiol-Michael addition reactions with two different acrylates: a hydrophobic perfluorinated acrylate and a hydrophilic hydroxy acrylate. After incubating the objects in a reaction medium for 24 hours, the desired modifications were achieved.

Reaction media:

i. 10 mL ethanol
ii. 0.05 mL triethyl amine, TEA (catalyst)
iii. Acrylate, either:

- Hydrophilic: 164 mg [2-(Methacryloyloxy)ethyl]dimethyl-(3-sulfopropyl)ammonium hydroxide

-or-

- Hydrophobic: 0.5 mL 1*H*,1*H*,2*H*,2*H*-Perfluorodecyl acrylate

Chemical pattering

For other unmodified OSTE (see recipe below) structures printed, a hydrophilic-hydrophobic chemical pattern was created on the surface of 3D objects. We printed macroporous truncated pyramids (**Fig. S1A**) and 3D masks (**Fig. S1B**) using a base layer cure time of 60 seconds, followed by subsequent layers cured for 10 seconds each at full light source power, while maintaining a layer thickness of 50 µm. The printing session lasted for 2.5 hours. After printing, we submerged the structures in acetone for 24 hours to remove any remaining resin residues (**Fig. S1C**). The patterning protocol was conducted the following day for approximately one hour. The structure was placed in a Reynolds-wrap container with a 1-2 mm layer of acetone to prevent sample drying. A 3D photomask, wet with acetone and containing circular holes with a diameter of 2 mm, was placed on the truncated pyramid. Then, 300 µL of a hydrophilic mixture

was distributed into all 9 mask openings, followed by a 2-minute exposure to UVC light (UVO Cleaner, model 42-220, Jetlight Co. Inc, USA). The hydrophilic mixture was composed of 1.35 mL of acetone, 0.15 mL of propenol, and 6.1 mg of 2,2-Dimethoxy-2-phenylacetophenone (photoinitiator). After illumination, the structure was immediately immersed in fresh acetone. The remaining surface of the cube was made hydrophobic by applying a solution of 7.5 mL acetone, 0.0375 mL triethyl amine (TEA), and 0.175 mL 1H,1H,2H,2H-Perfluorodecyl acrylate the following day. After the hydrophobization process, the sample was washed with acetone for 24 hours. An additional wash was performed 10 minutes before the critical point drying process to remove any remaining residues. The final structure was superhydrophobic in its bulk, while its surface consisted of water-adherent hydrophilic circles in a superhydrophobic matrix. See additional proof of the patterned adhesion in the supporting video file **V1_WettabilityPattern.mp4**.

Resin recipe used for printed of truncated pyramids and 3D photo-mask.

Pentaerythritol tetrakis(3-mercaptopropionate) (PETMP)	32.4 wt%	12.94 g
tri(ethylene glycol) divinyl ether (TEG)	17.7 wt%	7.06 g
Polyethylene glycol 200 (PEG200)	50 wt%	20 g
Irgacure 819 (2 % mol to thiol)		0.282 g
Sudan I (0.025 wt% of total ink)		0.010 g
TEMPO (0.01 wt% of total ink)		0.004 g

Total weight of PETMP + TEG + PEG200 = 40 g. Stoichiometric ratio: [thiol]/[alkene] = 1.5.

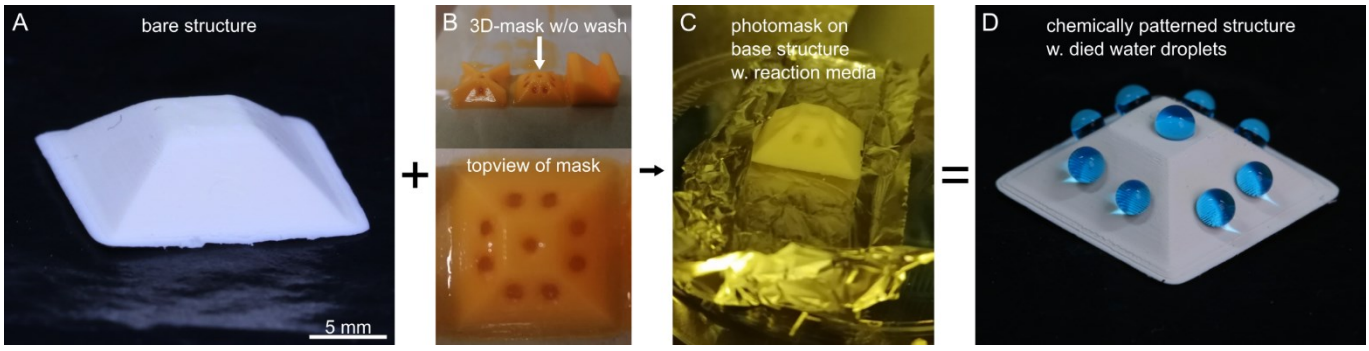

Fig. S1 Stages of Chemical Patterning on a 3D Object. **A)** Displays the initial structure as printed using off-stoichiometric thiol-ene chemistry. **B)** Shows the photopatterning mask, made from the same resin, used for precise chemical modifications. **C)** Depicts the photomask positioned on the structure in an acetone bath, where a hydrophilic reactive solution is applied to the mask openings, and subsequently exposed to UVC light. **D)** Illustrates the final structure post-hydrophobization, highlighting the established wettability pattern through selective water adhesion on hydrophilic areas.

Critical point drying

Finally, the structures were dried using supercritical drying to prevent the collapse of the macroporous structures of the 3D-printed objects.[1] The objects were immersed in acetone and then placed in a supercritical drying chamber (Leica EM CPD030 or CPD300, Germany). The process was run in manual mode with at least 12 solvent exchange cycles.

Methacrylate reference material

For the methacrylate-based ink utilized in this study, the compositions and printing details were: The monomer composition consisted of 30 wt% hydroxyethyl methacrylate (HEMA), 20 wt% ethylene glycol dimethyl acrylate (EDMA), 25 wt% cyclohexanol, 25 wt% 1-decanol, and 1 wt% Irgacure 819. The curing layer time was 40 seconds, while the base curing time was 60 seconds. The layer thickness was 100 micrometers, and the light intensity was set to 50 percent. After printing, the 3D objects were removed from the build platform and washed in acetone for 24 hours to remove unreacted monomers and porogens. Supercritical drying was used to dry the 3D printed objects.

Characterization

Scanning electron microscopy and surface porosity

The macroporous structure of the 3D-printed objects was characterized using a scanning electron microscope (Zeiss LEO 1530, Germany) at an operating voltage of 5 kV. Prior to SEM measurements, a 7 nm thick layer of platinum was coated on the samples. Both surface and cross-sectional SEM images were acquired to estimate surface porosity using Matlab 2022b. Porosity was estimated from a binary conversation that utilized adaptive thresholding (**Fig. S2**)

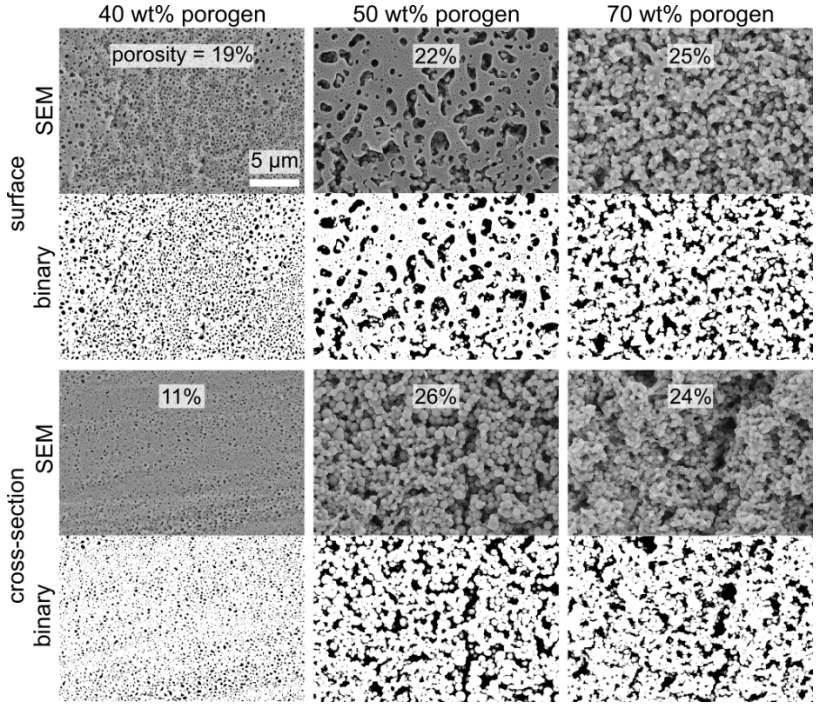

Fig. S2 Scanning electron micrographs (SEM) illustrating the variation in surface and cross-section porosity are presented. The binary conversion results are shown below each SEM image.

Pore size distribution

Pore diameter distributions for the different porogen fractions were also characterized (see Fig. S3). Distributions were calculated using ImageJ/Fiji's 'Analyze Particles...' plug-in on the binary images of Fig. S2 and the area converted to an effective diameter using the equation for a circle. Particles smaller than 3 pixels were excluded as noise.

	40% porogen	**50% porogen**	**70% porogen**
Average	113 nm	256 nm	221 nm
Standard deviation	58 nm	360 nm	307 nm
Median	101 nm	112 nm	106 nm

Table S1 Effective pore diameter summary statistics

Note that the mean and median values provided in **Table S1** are highly sensitive to the thresholding process due to the heterogeneity of the structure. However, based on the pore size distribution in **Fig. S3**, it is clear that the average pore size is above the macroporous polymer defining threshold of 50 nm.

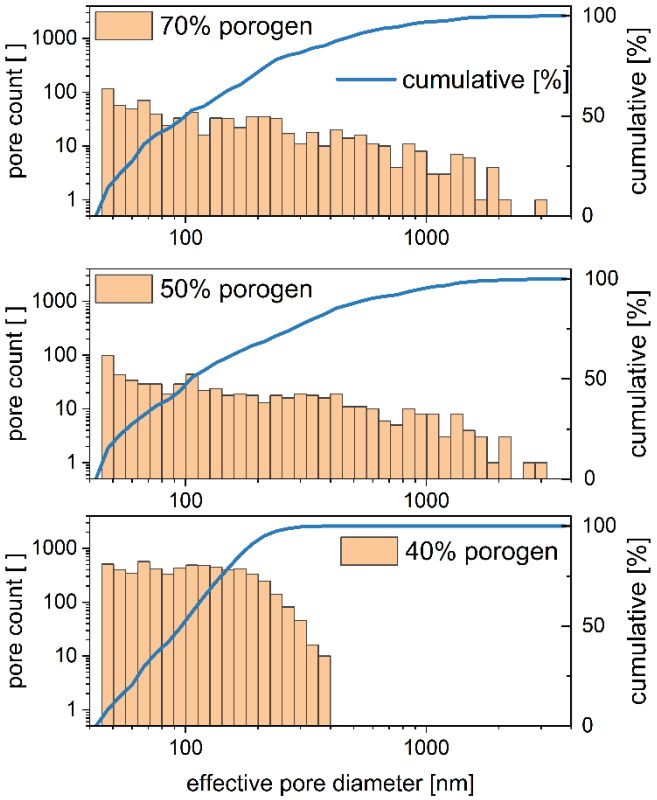

Fig. S3 The pore-size distribution for three different porogen fractions.

Mechanical testing

The mechanical properties of our 3D-printed cubes, each measuring 5 × 5 × 5 mm^3, were evaluated using the AGS-X Universal Tester from Shimadzu Inc., Japan, in compression test mode. The specimens were compressed in the z-direction at a rate of 0.25 mm/min until fracture was observed in the stress-strain plot. A pristine macroporous cube was used for each test. The sample's compressive strength and Young's modulus were determined by analyzing the strength at the fracture point and the slope of the linear region of the stress-strain curve in Origin 2022b

The cyclic compression test was conducted following a similar procedure, but with a compression rate of 10% per minute. To calculate energy recovery, each stress value was multiplied by the size of each strain step and summed across all strain values for both the loading and unloading curves. Microsoft Excel was used to approximate the area of the loading and unloading curves. The energy recovery was defined as the summation of the unloading curve divided by that of the loading curve.

A complete loading-unloading cycle of this process, accelerated to 50 times the normal speed, is available for viewing in supplementary video file **V2_ThioleneLoadingUnloading_50x.avi**.

Wetting characterization

The wetting properties of both as-printed and modified samples were characterized using the DSA25S drop shape analyzer (Krüss, Hamburg, Germany). The characterization was performed with 5x5x5 mm^3 cubes (50% porogen), using deionized (DI) water.

For both the unmodified and hydrophilic samples, a 5 µL droplet was placed on the cube, and its absorption was recorded on video. The study quantified the wicking dynamics by characterizing the apparent contact angle as a function of time. The angles were calculated using Tracker 6.0.x by tracking the (x,y)-coordinates of the two triple points and two points on the surface at approximately 10% of the droplet height.

For the hydrophobic samples, advancing and receding contact angles were characterized using the inflation/deflation technique.[2] Initially, a 2 µL droplet was formed in mid-air and then gently brought into contact with the surface. The syringe needle was centered and positioned less than 1 mm from the substrate to minimize disturbance to the droplet's shape near the contact line and allow room for deflation. The droplet was inflated at a rate of 0.2 µL/s until it reached a volume between 10 and 20 µL. This process was recorded at a frame rate of 1 fps. Finally, the droplet was deflated using the same pumping and frame rates. **Fig. S4** provides an example of the superhydrophobic properties.

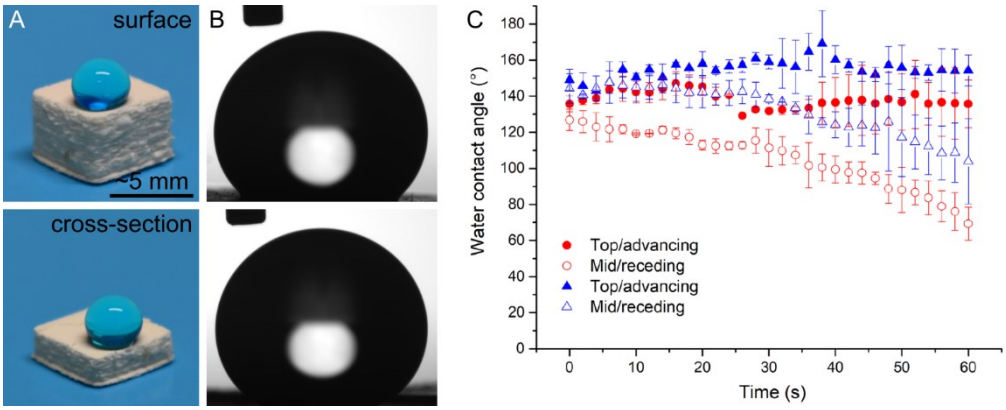

Fig. S4 Wettability Characterization of Superhydrophobic Cube. **A)** Illustrates the apparent contact angle through a tilted photo with a dyed water droplet and side-view imaging via a drop shape analyzer. **B)** Shows advancing and receding contact angles on the cube's top and cross-sectional surfaces.

Raman spectroscopy

Raman spectra were obtained using a Senterra Raman microscope (Bruker Optics, Ettlingen, Germany) with an excitation laser at λ = 532 nm and 0.2 mW output power. The range of collection was 50–3640 cm^{-1}. An Olympus MPLAN 20× objective, NA 0.5 (Olympus, Tokyo, Japan), was used to visualize the sample, focus the excitation beam, and collimate backscattered light. Data acquisition and spectra analysis were performed using Bruker OPUS software 7.8. Origin 2022b was used for background correction using a 7–10-point b-spline fitting. **Fig. S5** shows the raw Raman shifts from 2000-2800 cm^{-1}. **Fig. S5A** shows the effect of off-stoichiometric thiol:alkene ratios (1.25:2.0 and 1.50:2.0), with the free thiol bonds around 2530-2610 cm^{-1}. In **Fig. S5B**, Raman spectra of the modified and unmodified polymer cubes (5 x 5 x 5 mm3) are shown. Hydrophobic (PFDA) and hydrophilic (HEA) were used for post-polymerization modifications. The highlighted area shows a peak for the unmodified cube's unreacted thiol moieties at 2575 cm^{-1}.

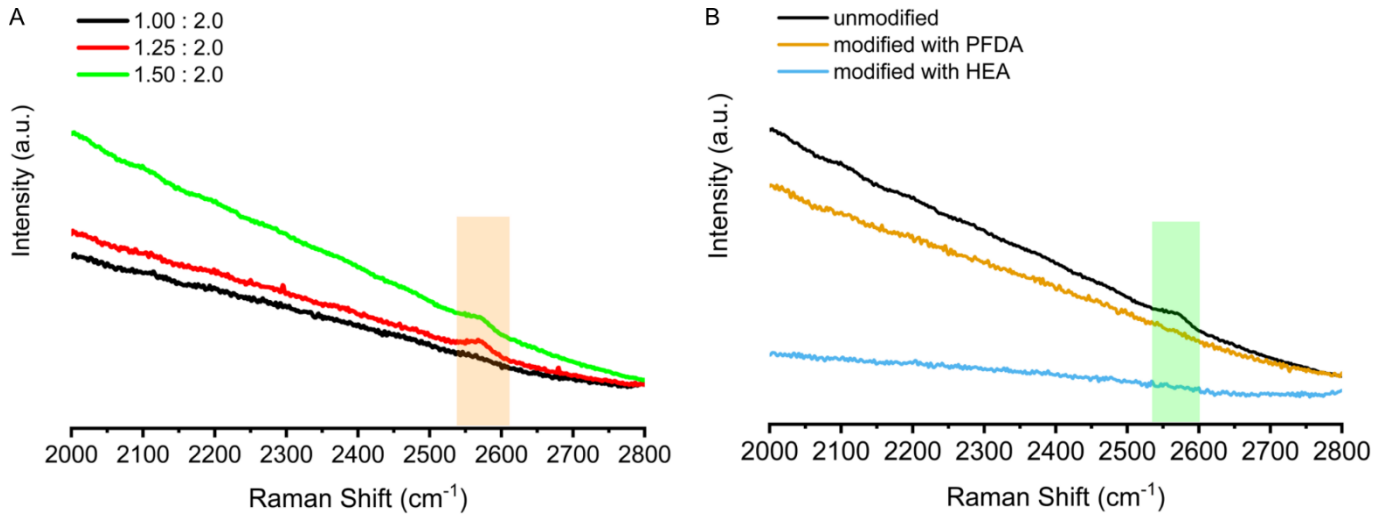

Fig. S5 Raman spectra of the polymer cubes (5 x 5 x 5 mm3) printed using **A)** thiol-ene resin for different off-stoichiometric ratios of thiol:ene (PETMP:TEG) are 1.00:2.0, 1.25:2.0, 1.50:2.0, respectively, and **B)** modified and unmodified polymer cubes printed with off-stoichiometric ratios of thiol:ene (PETMP:TEG) is 1.50:2.0. Post-polymerization modifications were performed using hydrophobic (PFDA) and hydrophilic (HEA) compounds. The highlighted area indicates the presence of residual/unreacted thiol moieties at approximately 2575 cm^{-1}.

Additional explorations

Identification of porogen candidates based on solubility

Porogens are a critical component in obtaining porous polymers for specific applications. Porogen solvents control the stability, selectivity, and permeability of the resulting porous polymers. The choice of porogen is often based on prior knowledge and published recipes which consider physicochemical characteristics such as solubility parameters, polarity index, partition coefficient, and dipole moment. Several criteria that must be met for a solvent to be employed as a porogen are as follows: First, the porogenic solvents must be miscible with each other when combined with the monomers and crosslinkers to form a homogeneous solution. However, the porogenic solvent should be immiscible with the resulting polymer. Second, the porogenic solvent should not react or polymerize with the monomer or other components of the polymerization mixture, or polymerize itself. Thirdly, when 3D printing porous polymers, it is important to ensure that the viscosity and evaporation of the porogen are compatible with the manufacturing procedure[3,4].

To investigate the appropriate solvent and solvent ratio, we prepared inks with various solvents and solvent ratios. The ink composition consisted of pentaerythritol tetrakis(3-mercaptopropionate) (PETMP), tri(ethylene glycol) divinyl ether (TEG), and Irgacure 819 (phenyl bis(2,4,6-trimethyl benzoyl)-phosphine oxide). We added TEG at twice the molar concentration of PETMP, while Irgacure 819 was added at 2% mol to thiol (8%). Porogen solvent was added to either 50 wt% or 70 wt% of the mixture, which was prepared in a black glass vial to prevent exposure to UV light. After sonication for 15 minutes at 25°C, the solubility behavior of crosslinkers with different porogen solvents at varying fractions was summarized in **Table S2** at room temperature (RT).

Porogen Solvent	**Solubility at RT**	**Solubility at RT**
	50 wt%	**70 wt%**
PEG200	**+**	**+**
THF	**+**	**+**
1-Propanol	**-**	**-**
DGDE	**+**	**+**
Toluene	**+**	**+**
Ethylene glycol	**-**	**-**
PEG : DGDE (1:1)	**+**	**+**
PEG : THF (1:1)	**+**	**+**
1-Decanol	**-**	**-**
Cyclohexanol	**+**	**-**
PEG : Cyclohexanol (1:1)	**-**	**+**
2-propanol	**-**	**-**
Cyclohexanol : DGDE (1:1)	**+**	**+**
DMA	**+**	**+**
DMF	**+**	**+**
DMSO	**+**	**+**

Table S2 Solubility results of resins prepared with PETMP : TEG (1 : 2) and photoinitiator at different porogen fractions and compositions.

Identification of phase-separation-inducing porogens by bulk photopolymerization

To test the ability to demonstrate polymerization-induced phase separation at a high throughput, we utilized bulk polymerization. We extracted polymeric cylinders, each 3 mm thick, from a PTFE mold after bulk photopolymerization of resins incorporating a miscible porogen using a Biolink™ BLX UV Crosslinker (Vilber Louvert, France) at an intensity of 5.0 mW/cm^2 with UVA light at a wavelength of 365 nm. The curing stage lasted for 15 minutes. The cylinders were immersed in acetone for 24 hours to remove any unreacted monomer and porogen. Supercritical drying was then used to preserve the integrity of the macroporous structures. **Fig. S6A** shows photographs of the experimental results. The samples appear white due to porosity-induced scattering. The PerkinElmer Lambda 35 from Waltham-USA was used as the UV-Vis spectrometer to measure the UV-Visible light transmittance of the 3 mm thick polymeric cylinders. A bare glass slide was used as a reference to record the background signal. The transmittance results for the selected samples are shown in **Fig. S6B**. Additionally, the compressive strength of the samples was briefly tested, as shown in **Fig. S6C**.

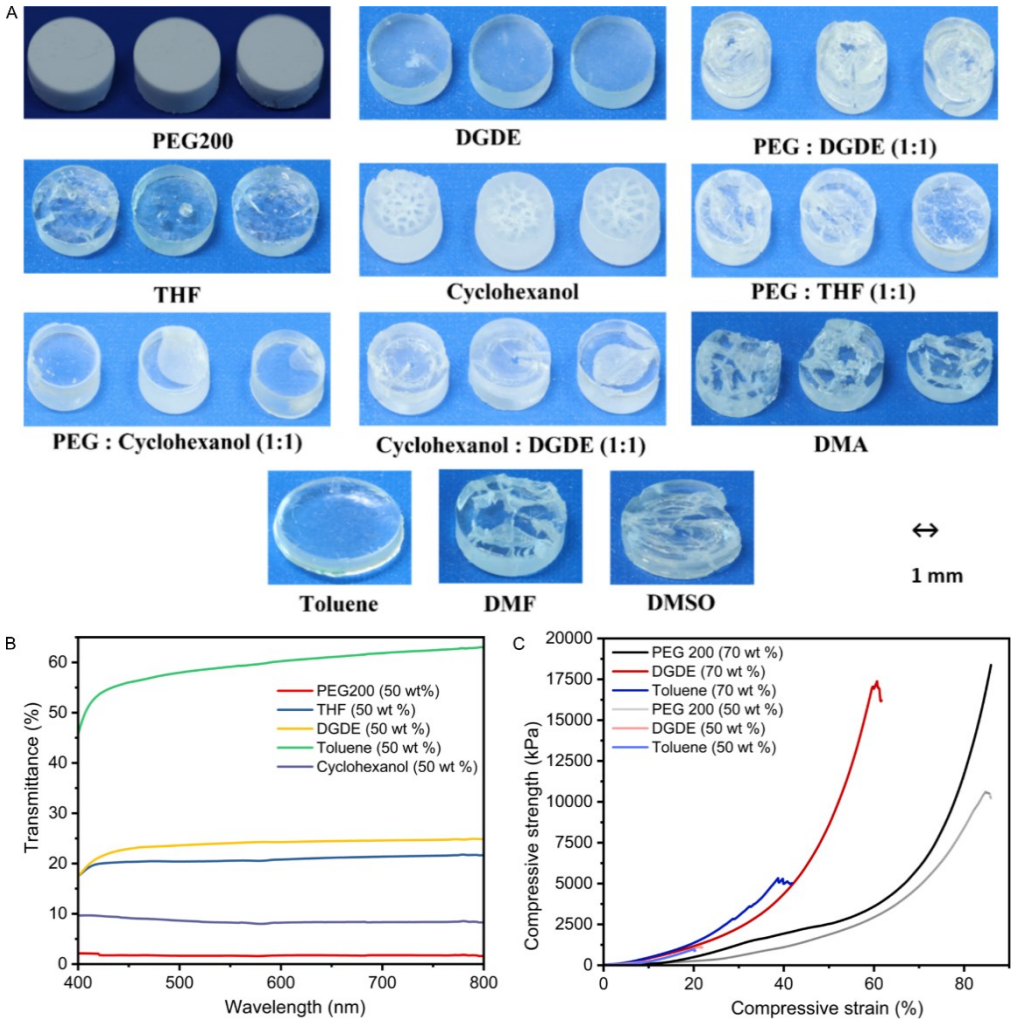

Fig. S6: Influence of variation in porogen type and fraction. **A)** Images of the resulting polymers prepared with the resin containing crosslinkers (PETMP: TEG (1:2), PI) and 50 wt% of porogen are shown. The scale bars are 1 mm and are the same for all images. **B)** The resulting polymers prepared with the resin containing crosslinkers (PETMP : TEG (1 : 2)), PI, and 50 wt% of the porogen have transmittance spectra. **C)** The mechanical properties of the porous thiol-ene polymers are influenced by 50 and 70 wt% of porogen solvents, as shown by the stress-strain curves.

References

1 Z. Dong, H. Cui, H. Zhang, F. Wang, X. Zhan, F. Mayer, B. Nestler, M. Wegener and P. A. Levkin, *Nat Commun*, 2021, **12**, 247.

2 T. Huhtamäki, X. Tian, J. T. Korhonen and R. H. A. Ras, *Nature Protocols*, 2018, **13**, 1521–1538.

3 F. R. Mansour, S. Waheed, B. Paull and F. Maya, *Journal of Separation Science*, 2020, **43**, 56–69.

4 S. Yu, F. L. Ng, K. C. C. Ma, A. A. Mon, F. L. Ng and Y. Y. Ng, *Journal of Applied Polymer Science*, 2013, **127**, 2641–2647.